Biol Trace Elem Res (2016) 169:94–105
DOI 10.1007/s12011-015-0381-9

The Protective Effect of Bafilomycin A1 Against Cobalt Nanoparticle-Induced Cytotoxicity and Aseptic Inflammation in Macrophages In Vitro

Songhua Wang[1] · **Fan Liu**[2] · **Zhaoxun Zeng**[1] · **Huilin Yang**[1] · **Haitao Jiang**[3]

Received: 29 January 2015 / Accepted: 21 May 2015 / Published online: 9 June 2015

Abstract Co ions released due to corrosion of Co nanoparticles (CoNPs) in the lysosomes of macrophages may be a factor in the particle-induced cytotoxicity and aseptic inflammation accompanying metal-on-metal (MOM) hip prosthesis failure. Here, we show that CoNPs are easily dissolved under a low pH, simulating the acidic lysosomal environment. We then used bafilomycin A1 to change the pH inside the lysosome to inhibit intracellular corrosion of CoNPs and then investigated its protective effects against CoNP-induced cytotoxicity and aseptic inflammation on murine macrophage RAW264.7 cells. XTT {2,3-bis (2-methoxy-4-nitro-5-sulfophenyl)-5-[(phenylamino) carbonyl]-2H-tetrazolium hydroxide} assays revealed that bafilomycin A1 can significantly decrease CoNP-induced cytotoxicity in RAW264.7 cells. Enzyme-linked immunosorbent assays showed that bafilomycin A1 can significantly decrease the subtoxic concentration of CoNP-induced levels of pro-inflammatory cytokines (tumor necrosis factor-α, interleukin-1β, and interleukin-6), but has no effect on anti-inflammatory cytokines (transforming growth factor-β and interleukin-10) in RAW264.7 cells. We studied the protective mechanism of bafilomycin A1 against CoNP-induced effects in RAW264.7 cells by measuring glutathione/oxidized glutathione (GSH/GSSG), superoxide dismutase, catalase, and glutathione peroxidase levels and employed scanning electron microscopy, transmission electron microscopy, and energy dispersive spectrometer assays to observe the ultrastructural cellular changes. The changes associated with apoptosis were assessed by examining the pAKT and cleaved caspase-3 levels using Western blotting. These data strongly suggested that bafilomycin A1 can potentially suppress CoNP-induced cytotoxicity and aseptic inflammation by inhibiting intracellular corrosion of CoNPs and that the reduction in Co ions released from CoNPs may play an important role in downregulating oxidative stress in RAW264.7 cells.

Keywords Cobalt nanoparticle · Inflammation · Intracellular solubilization · Lysosome · Toxicity

Introduction

Metal-on-metal (MOM) hip replacements were reintroduced in the 1990s as an attractive alternative bearing surface in total hip arthroplasty (THA), due to their minimal wear debris as compared to conventional metal-on-polyethylene (MOP) bearings [1, 2]. Wear is an inevitable consequence of total joint arthroplasty [3]. MOM bearings made of a cobalt −chromium (CoCr) alloy generate a large amount of metal particles and ions in vivo [2]. Metal particles obtained from revisioned periprosthetic tissues were smaller than 50 nm, and the number of wear particles was 13–500 times higher than that seen in MOP bearings [4, 5].

To date, more than 1,000,000 patients worldwide have undergone MOM hip replacement. However, this approach has led to the development of unacceptable side effects, such as

SonghuaWang and Fan Liu contributed equally to this work.

✉ Fan Liu
fanliu1957@163.com

[1] Department of Orthopedics, The First Affiliated Hospital of Soochow University, Shizi Street, Suzhou 215006, Jiangsu Province, People's Republic of China

[2] Department of Orthopedics, The Affiliated Hospital of Nantong University, 20 West Temple Road, Nantong 226001, Jiangsu Province, People's Republic of China

[3] Department of Orthopedics, The First People's Hospital of Taizhou City, Taizhou, Jiangsu Province, People's Republic of China

pseudotumors, extensive necrosis, early osteolysis, and failure due to aseptic loosening [6, 7]. These unexplained adverse biological reactions were mainly attributed to cytotoxicity and tissue inflammatory reactions following the release of Co and Cr ions from the MOM implant [8, 9]. Dalal et al. [10] reported that cobalt–alloy particles result in greater toxicity and production of more inflammatory cytokines than do titanium–alloy and zirconium–alloy-based particles in vitro.

Wear metal nanoparticles are exclusively phagocytized by macrophages and are stored in the lysosome; the low pH inside the lysosome solubilizes metal nanoparticles easily [11–13]. Recent studies revealed that cytotoxicity was observed only with Co [8, 9]; it is possible that Co more easily undergoes intracellular corrosion than does Cr, and that the release of high levels of these ions increases intracellular ROS levels [12, 14].This suggests that it is the soluble products released from wear-particle corrosion, rather than the particles themselves, that lead to cytotoxicity and inflammatory reactions. We hypothesized that the cytotoxicity and inflammation that follows the intracellular corrosion of Co is the reason for the unexplained adverse biological reactions to MOM implants.

Pro-inflammatory cytokines, such as tumor necrosis factor-α (TNF-α), interleukin-1β (IL-1β), and interleukin-6 (IL-6), have been found in the tissue surrounding failed implants, and are considered as factors in bone resorption [15, 16]. Both soluble Co and Co-Cr-Mo alloy particles can stimulate macrophages to release inflammatory cytokines in vitro, but Cr did not induce significant secretion of TNF-α, IL-1β, and IL-6 [17]. Consequently, we conjectured that the Co ions contribute to the extensive osteolysis and elevated levels of inflammatory cytokines surrounding failed implants.

Bafilomycin A1 is a strong inhibitor of the vacuolar type H^+-ATPase and can prevent a decrease in pH within lysosomes; thereby significantly reducing the intracellular corrosion of Co [13, 18]. Therefore, we hypothesized that bafilomycin A1 may hold potential for suppressing CoNP-induced cytotoxicity and aseptic inflammation in murine macrophage RAW264.7 cells. Herein, we investigated the protective effects of bafilomycin A1 against CoNP-induced cytotoxicity and aseptic inflammation in murine macrophage RAW264.7 cells, in order to elucidate the possible mechanisms underlying the adverse biological reactions that follow MOM hip replacement.

Materials and Methods

Materials

CoNPs (median size 50 nm), bafilomycin A1, XTT, and phenazine methosulfate (PMS) were purchased from Sigma-Aldrich (St. Louis, MO, USA). CoNPs samples were heat-sterilized by baking at 250 °C for 3 h [19]. All the particles were free of endotoxins, as measured using a Limulus amebocyte lysate (LAL) assay kit (Charles River Laboratories, Wilmington, MA, USA) at a detection level of 0.25 % EU/mL. Stock solutions of CoNPs were prepared at a concentration of 100 mM in ultrapure water. The stock solutions were sonicated intermittently six times for 30 min [20]. After ultrasonification, the CoNP solutions were analyzed by transmission electron microscopy (TEM; JEM-2010, JEOL, Tokyo, Japan; Fig. 1). The stock solutions were freshly diluted with culture medium to the test concentrations. Cobalt chloride (Co^{2+}) and HCl were purchased from Sinopharm Chemical Reagent (Shanghai, China). Cobalt chloride (Co^{2+}) was prepared at a concentration of 100 mM using ultrapure water and sterilized using a 0.2-μm syringe filter (Corning, New York, USA). Dulbecco's modified Eagle's medium (DMEM), fetal bovine serum (FBS), penicillin/streptomycin, and trypsin were purchased from Invitrogen (Paisley, UK). All murine-specific ELISA kits were purchased from R&D System (Minneapolis, MN, USA). A total glutathione/oxidized glutathione (T-GSH/GSSG, A061-2), total-, copper/zinc-, and manganese superoxide dismutase (T-SOD, CuZnSOD, MnSOD, A001-3), catalase (CAT, A007-2), and co-substrate glutathione peroxidase (GPx, A005) assay kits were purchased from Nanjing Jiancheng Bioengineering Institute (Nanjing, China). Goat anti-rabbit IgG conjugated with horseradish peroxidase (GAR-HRP), polyclonal antibodies against Akt, phospho-Akt (Ser473), cleaved caspase-3, and β-actin were all purchased from Cell Signaling Technology Inc. (Danvers, MA, USA). Tissue culture dishes were obtained from Corning

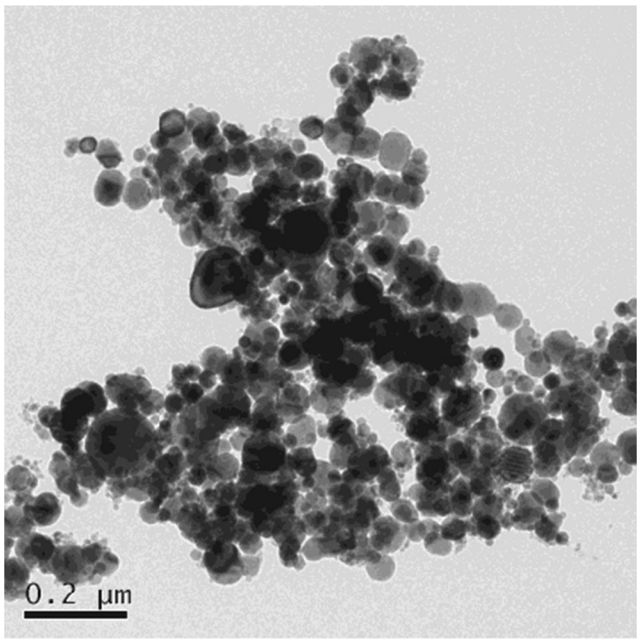

Fig. 1. Transmission electron microscopy images of cobalt nanoparticles (CoNPs) after ultrasonification

(New York, NY, USA). Other materials were purchased from Sigma-Aldrich.

Cell Culture

The murine macrophage RAW264.7 cell line was obtained from the China Center for Type Culture Collection (Shanghai, China). RAW264.7 cells were cultured in DMEM medium containing 10 % FBS and 1 % penicillin/streptomycin. The cells were kept at 37 °C in a humidified atmosphere of 5 % CO_2. RAW264.7 cells were randomly divided into four groups: blank control group, CoNPs group, CoNPs +8 nM bafilomycin A1group, and CoNPs +16 nM bafilomycin A1 group.

Cell Viability Assays

Effects of CoNPs, Co^{2+}, and bafilomycin A1 on the viability of RAW264.7 cells were evaluated using the XTT assay. Cells (1.5×10^4 cells/well) were plated into 96-well tissue culture plates and exposed to CoNPs, Co^{2+} (0–800 μM), and bafilomycin A1 (8 nM and 16 nM) for 4, 24, and 48 h. Culture medium served as the control in each experiment. In order to examine the protective effects of bafilomycin A1 on the viability of RAW264.7 cells co-cultured with CoNPs, the cells were pre-incubated for 4 h in the presence of different concentrations of bafilomycin A1, and subsequently, the cells were exposed to 50 μM CoNPs for 24 h. XTT was prepared at 1 mg/mL in prewarmed (37 °C) medium without serum. PMS was prepared at 5 mM (1.53 mg/mL) in phosphate-buffered saline (PBS). Fresh XTT and PMS were mixed together at the appropriate concentrations. Thereafter, 50 μL of this mixture (final concentration, 50 μg of XTT and 0.38 μg PMS per well) were added to each well and the cells were incubated for 4 h at 37 °C. Optical density of this solution was measured at 450 nm using a microplate reader (Wellscans MK3, Thermo Lab Systems, Vantaa, Finland). Cell viability rates were expressed as percent of the control; from this, the 50 % inhibitory concentration (IC50 value) [2] was calculated.

Ion Release Under Different pH Values

To evaluate the level of Co ions released from CoNPs in medium under different pH values, CoNPs (50 μM, corresponding to the IC50) were incubated in cell-free and serum-free DMEM medium at a pH of 7.2, 6.0, 5.0, or 4.0. The pH of 7.2 is the same as the pH level in serum-free DMEM medium and the pH of 4.0 is the same as that found within lysosomes in macrophages [12]. The pH was adjusted to the appropriate value by the addition of 0.5 M HCl. After 4, 24, or 48 h at 37 °C, the particles were then removed from the medium by centrifugation (4000×*g* for 20 min). The particle-free supernatants were tested for levels of Co^{2+} by inductively coupled plasma-mass spectrometry (ICP-MS; 7500A Series; Agilent, Santa Clara, CA, USA), and these levels were expressed as nanogram per milliliter (ppb).

Inhibition of Intracellular Solubilization of CoNPs by Bafilomycin A1

In order to examine the effects of inhibiting intracellular solubilization of CoNPs by bafilomycin A1, RAW264.7 cells were randomly divided into three groups: 50 μM CoNPs group, 50μMCoNPs + 8nMbafilomycin A1 group, and 50μMCoNPs + 16 nM bafilomycin A1 group. In the 50 μM CoNPs group, 2×10^5 RAW264.7 cells/well were plated into 24-well tissue culture plates. After attached, serum-free DMEM medium (pH = 7.2) containing 50 μM CoNPs was added into the plates and then incubated at 37 °C for 4, 24, and 48 h, in a 95 % humidified atmosphere with 5 % CO_2. In the other two groups, 2×10^5 RAW264.7 cells/well were plated into 24-well tissue culture plates, which were pre-incubated with different concentrations of bafilomycin A1 (8 nM or 16 nM) for 4 h. After attached, serum-free DMEM medium (pH 7.2) containing 50 μM CoNPs were added into the plates and then incubated under the same conditions. Finally, RAW264.7 cells were washed thrice with PBS to eliminate CoNPs attached to the outside of the cells. After lysis, trypsinization, and centrifugation, we harvested the supernatant (cell extracts), tested the levels of Co^{2+} by ICP-MS (expressed as nanogram per milliliter [ppb]), and used the pellets for energy dispersive spectrometer (EDX) assays.

Analysis of Morphological Cell Changes

All four groups of RAW264.7 cells were incubated as above for 24 h. The viability, morphology, spreading, and ultrastructural changes of the cells were analyzed by scanning electron microscopy (SEM) and TEM. For SEM analysis, RAW264.7 cells were seeded on a glass cover slip in 24-well plates at 1×10^5 cells/well, then washed with PBS to eliminate CoNPs attached to the outside of the cells. Cells were fixed for 60 min with 2.5 % glutaraldehyde and dehydrated in graded ethanol solutions. After sputter-coating with gold, the samples were observed using a Hitachi S-4700 scanning electron microscope (Tokyo, Japan), under an accelerating voltage of 1 kV. For TEM analysis, 5×10^6 RAW264.7 cells/well were plated into 6-well tissue culture plates. Cells were washed with PBS and fixed with 2.5 % glutaraldehyde and 1 % osmium tetroxide for 3 h, and then dehydrated using graded concentrations of ethanol. After infiltration and embedment in epoxy resin at 60 °C for 48 h, the ultra-thin sections were stained with lead citrate and examined by TEM (H-600, Hitachi, Tokyo, Japan; accelerating voltage of 100 kV).

Detection of Cytokines

Subtoxic concentrations of CoNPs (20 μM, below the IC50) were selected to evaluate the release of pro-inflammatory cytokines. For all four groups, RAW264.7 cells (5×10^5 cells/well) were plated into 24-well plates and incubated with 20 μM CoNPs using the same methods as above. At 24 h after the treatment, the supernatants of each well were removed and added to 96-well ELISA plates to assess cytokine levels; the cells themselves were washed with PBS and lysed ultrasonically on ice for 30 s and centrifuged at 15,000×*g* for 15 min. These cell extracts were used to assess antioxidant enzymes as described below. TNF-α, IL-1β, IL-6, transforming growth factor-β (TGF-β), and interleukin-10 (IL-10) levels were measured using ELISA test kits. The ELISA kits for murine TNF-α, IL-1β, IL-6, TGF-β, and IL-10 were purchased from R&D Systems (Minneapolis, MN, USA). The optical density of samples was determined at 450 nm with a reference filter of 630 nm using a microplate reader. The concentration (pg/mL) of TNF-α, IL-1β, IL-6, TGF-β, and IL-10 were calculated according to the standard curve provided in the ELISA kits. The cytokines levels were expressed as pictogram (pg) per milliliter.

Measurement of Non-Enzymatic and Enzymatic Antioxidant Defense Systems

The cell extracts acquired above were used for spectrophotometric measurements of non-enzymatic and enzymatic antioxidant defense systems. The T-GSH/GSSG levels and enzymatic activities of T-SOD, CAT, and GPx were detected according to the manufacturer's protocol using the corresponding diagnostic kits. Total GSH/GSSG levels were determined enzymatically by the 5, 5′-dithiobis (2-nitrobenzoic acid)–glutathione reductase method as described by Mak et al. [21, 22]. T-SOD activity was assayed using the xanthine/xanthine oxidase method based on the production of O^{2-} anions [23]. The CAT activity was measured based on the hydrolysis reaction of hydrogen peroxide (H_2O_2) with CAT, which could be terminated by molybdenum acid (MA) to produce yellow MA H_2O_2 complex [24]. The GPx activity was assayed by method of Rotruck et al. [25] and measured based on the principle that oxidation of GSH and hydrogen peroxide (H_2O_2) could be catalyzed by GPx to produce GSSG and H_2O. The T-GSH/GSSG levels were expressed as micromole (μM) per milligram of protein, and enzyme activities were expressed as unit (U) per milligram of protein.

Western Blot Analysis

Cells were pre-incubated for 4 h in the presence of different concentrations of bafilomycin A1 (0, 8, and 16 nM), and subsequently, the cells were exposed to 50 μM CoNPs or vehicle for 24 h. The treated cells were washed twice with ice-cold PBS and harvested in a lysis buffer (20 mM HEPES, 10 mM EDTA, 100 mM NaF, 10 mM sodium pyrophosphate, 1 mM Na3VO4, 1 % (*v*/*v*) Nonidet P-40, 1 mM phenylmethylsulfonyl fluoride, and 0.1 mg/mL aprotinin at pH 7.5), and then subjected to SDS-PAGE and Western blot analysis with anti-pAKT, anti-AKT, and anti-caspase-3, respectively. Anti-β-actin antibody was used as a loading control to ensure that protein inputs in each group were similar.

Statistical Analysis

Statistical analyses were performed using SPSS software. Experiments were performed in triplicates, and the data presented are reported as mean ± standard deviation (SD). Statistical analysis of the data was performed using one-way analysis of variance (ANOVA), followed by Dunnet's test to evaluate the significance relative to control. Differences were considered statistically significant at $p < 0.05$.

Results

In this study, CoNPs and Co^{2+} inhibited the viability of RAW264.7 cells in a concentration- and time-dependent manner. The IC50 values at 24 h were approximately 50 and 400 μM for CoNPs and Co^{2+}, respectively. Treatment of cells with bafilomycin A1 at 8 and 16 nM had no cytotoxic effects on RAW264.7 cells (Fig. 2). Bafilomycin A1 showed clear protective effects on the viability of RAW264.7 cells co-cultured with CoNPs (50 μM; $p < 0.05$). The protective effects of bafilomycin A1 were significantly dose dependent ($p < 0.05$; Fig. 3).

The release of Co^{2+} from CoNPs (50 μM) in cell-free and serum-free DMEM medium under different pH values were analyzed by ICP-MS after 4, 24, and 48 h of incubation. A time- and pH-dependent increase in the release of Co^{2+} from CoNPs was found in the 50 μM CoNP group (Fig. 4). The intracellular solubilization of CoNPs after 4, 24, and 48 h of incubation with RAW264.7 cells in serum-free DMEM medium showed a time-dependent increase, and was dose dependently inhibited by bafilomycin A1; the difference between the two bafilomycin A1-treatment groups was statistically significant ($p < 0.05$; Fig. 5). Furthermore, we quantified the intracellular insoluble particulate fractions of Co using EDX. No characteristic Co peaks were seen in the control group, and these Co peaks were low in CoNPs group after 24 h of incubation with RAW264.7 cells in serum-free DMEM medium; however, the characteristic Co peaks increased in a dose-dependent manner in the two bafilomycin A1-treatment groups ($p < 0.05$; Fig. 6).

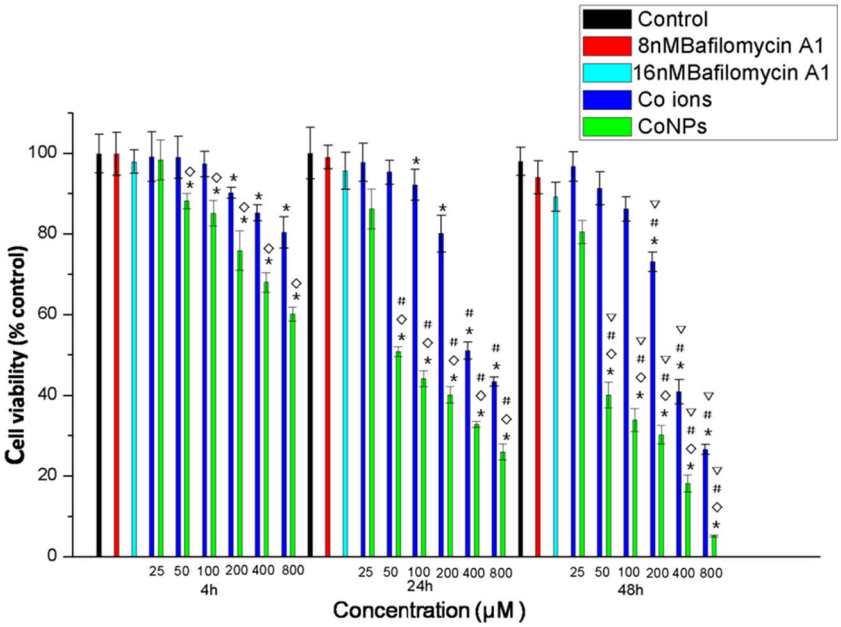

Fig. 2 Viability of RAW264.7 cells exposed to cobalt nanoparticles (CoNPs), cobalt chloride (Co^{2+}), and bafilomycin A1, as determined by XTT assay. Cells were treated with CoNPs (0 −800 μM), Co^{2+} (0−800 μM), and bafilomycin A1 (8 and 16 nM) for 4, 24, and 48 h. All data were expressed as mean ± SD of three independent experiments performed in triplicate. *$p < 0.05$ compared to control; ◊$p < 0.05$ compared to Co^{2+}; #$p < 0.05$ compared to 4 h; ∇$p < 0.05$, compared to 24 h

Using SEM, we observed that RAW264.7 cells had pseudopods when cultured in DMEM medium, but the cells became smaller and rounder and did not spread when co-cultured with CoNPs. In the two bafilomycin A1-treatment groups, RAW264.7 cells gradually redeveloped pseudopods, their morphology recovered, and they regained the ability to spread (Fig. 7a–d). From the TEM images (Fig. 7e–h), we observed that the number of lysosomes and vacuoles in RAW264.7 cells increased markedly after 24 h of incubation with CoNPs and that some cytoplasmic organelles had disappeared, as compared to the blank control group. The TEM images showed that CoNPs were enclosed in lysosomes and vacuoles in RAW264.7 cells. In the two bafilomycin A1-treatment groups, the TEM images showed a decrease in lysosomes and vacuoles and reappearance of cytoplasmic organelles in a bafilomycin A1 dose-dependent manner.

The levels of the TNF-α, IL-1β, IL-6, TGF-β, and IL-10 as detected by ELISA, are shown in Fig. 8. A subtoxic concentration (20 μM) of CoNPs provoked increased protein

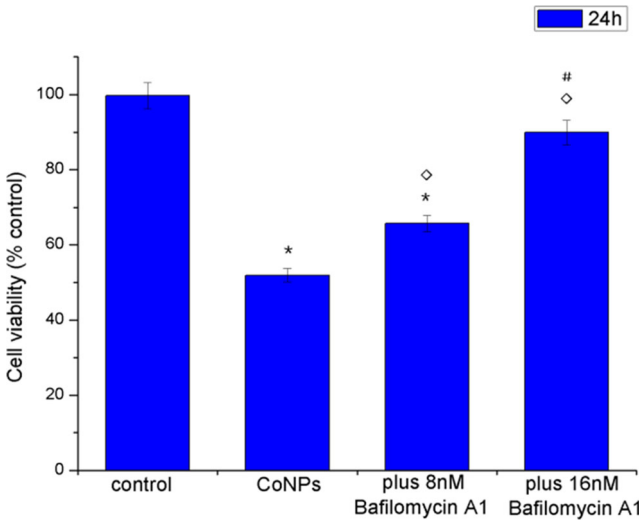

Fig. 3 Protective effects of bafilomycin A1 on the viability of RAW264.7 cells treated with cobalt nanoparticles (CoNPs), as determined by XTT assay. Cells were exposed to 50 μM CoNPs for 24 h. All data were expressed as mean ± SD of three independent experiments performed in triplicate. *$p < 0.05$ compared to control group; ◊$p < 0.05$ compared to CoNPs group; #$p < 0.05$compared to the 8 nM bafilomycin A1 group

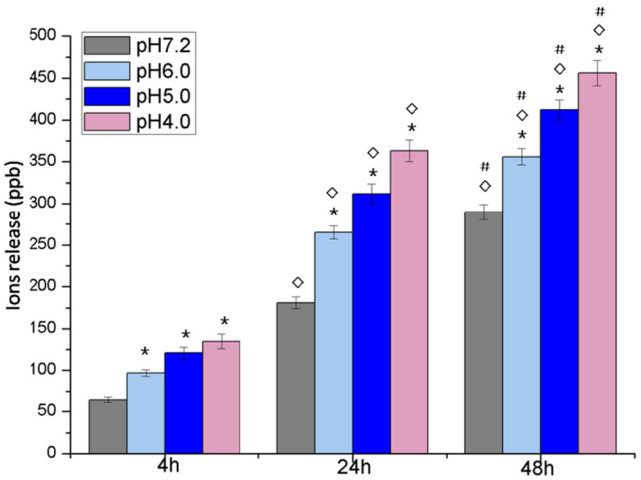

Fig. 4. Evaluate the level of Co ions released from cobalt nanoparticles (CoNPs) under different pH values after 4, 24, and 48 h of incubation. CoNPs (50 μM) were incubated in cell-free and serum-free DMEM medium at a pH of 7.2, 6.0, 5.0, or 4.0 for 4, 24, and 48 h. The levels of Co^{2+} in the medium supernatants were determined by inductively coupled plasma-mass spectrometry (ICP-MS). Values were showed as means ± SD of three independent experiments performed in triplicate. *$p < 0.05$ compared to pH 7.2; ◊$p < 0.05$ compared to 4 h; #$p < 0.05$ compared to 24 h

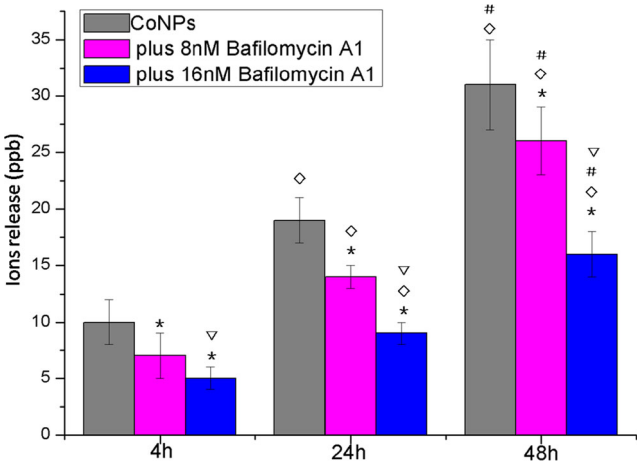

Fig. 5 Effects of bafilomycin A1 on the inhibition of intracellular solubilization of cobalt nanoparticles (CoNPs) analyzed by ICP-MS. CoNPs (50 μM) were phagocytized by RAW264.7 cells. After 4, 24, and 48 h of incubation in serum-free DMEM medium (pH 7.2), cell extracts were tested for levels of Co^{2+} by inductively coupled plasma-mass spectrometry (ICP-MS). All data were expressed as mean ± SD of three independent experiments performed in triplicate. A linear trend between the Co^{2+} release levels and the exposure time was observed. *$p < 0.05$ compared to CoNPs group; ◊$p < 0.05$ compared to 4 h; #$p < 0.05$ compared to 24 h; ∇$p < 0.05$ compared to 8 nM bafilomycin A1 group

expression of TNF-α, IL-1β, and IL-6 of RAW264.7 cells as compared with the levels in the blank control group at the 24-h time point ($p < 0.05$), while in the two bafilomycin A1-treatment groups, the expression of these three proteins were significantly suppressed in a dose-dependent manner ($p < 0.05$). The levels of TGF-β and IL-10 showed no obvious changes either when co-cultured with a subtoxic concentration of CoNPs or when treated with bafilomycin A1.

The T-GSH/GSSG level and the antioxidant enzymes T-SOD, CAT, and GPx were determined after a 24-h incubation with 20 μM CoNPs. As shown in Table 1, this subtoxic concentration of CoNPs significantly decreased the T-GSH level and the activities of antioxidant enzymes in RAW264.7 cells as compared to those in the blank control group ($p < 0.05$), while in the two bafilomycin A1-treatment groups, the T-GSH level and the activities of the antioxidant enzymes were recovered ($p < 0.05$).

Western blot analysis was used to estimate the changes associates with apoptosis by examining caspase-3 and pAKT protein levels in all groups, given that Akt activation protects murine RAW264.7 cells from CoNP-induced cell apoptosis and death. The effects of bafilomycin A1 on regulation of protein expression in murine RAW264.7 cells after exposure to CoNP were assessed by Western blotting. As shown in Fig. 9, compared with the control, the band intensity of pAKT on immunoblots was downregulated significantly, and cleaved caspase-3 (17kD) was upregulated after incubation with CoNP. However, treatment with bafilomycin A1 could reverse these changes in a dose-dependent manner.

Discussion

Given the concern about the possible adverse health effects of wear particles, the use of MOM for joint arthroplasty surgery has decreased markedly [26]. However, simply abandoning the use of MOM-THA does not solve the problem, as more than a million people have received these implants [9]. The mechanisms by which MOM wear debris interacts with the human body are not completely understood [26], although recent studies reported that adverse biological reactions were strongly correlated with Co [8, 9]. In this study, we evaluated the protective effect of bafilomycin A1 against CoNP-induced cytotoxicity and aseptic inflammation in RAW264.7 cells.

The classical MTT assay is widely used for evaluating cell viability, but it may lead to false interpretations due to interferences of the nanoparticles with assay components [27]. Here, the XTT cell viability assay was used to evaluate RAW264.7 cell viability. Our study showed that exposure to CoNPs and Co^{2+} decreased the viability of RAW264.7 cells, but the cytotoxic effects of CoNPs were stronger than those of Co^{2+}. This confirmed the findings of our previous study, which showed that the levels of extracellular Co^{2+} released from CoNPs in the culture medium were not sufficiently high to induce cell damage [2]. Comparing the solubilization level of CoNPs in the extracellular medium, as well as in the intracellular medium, is essential for elucidating the mechanisms of toxicity [13]. Our data showed that CoNPs were easily dissolved under a simulated lysosomal (pH 4.0) environment, but did not easily dissolve in medium mimicking the extracellular environment (pH 7.2).We hypothesized that intracellular corrosion of CoNPs occurred easily when these particles were phagocytized by cells and accumulated inside the acidic environment of the lysosome. Bafilomycin A1 is a strong inhibitor of the vacuolar type H^+-ATPase, which can change the acidic environment inside the lysosome [18]. To confirm this hypothesis, we used ICP-MS and EDX analyses to establish whether bafilomycin A1 can inhibit intracellular corrosion of CoNPs, by measuring the intracellular soluble Co ion concentrations [13], and the insoluble particulate fractions of Co in RAW264.7 cells, respectively, approximating the total CoNPs phagocytized in the cells. Our data verified that bafilomycin A1 could markedly inhibit intracellular corrosion of CoNPs and had a significant protective effect against CoNP-induced cytotoxicity. We conjectured that it was the soluble products released from intracellular corrosion of CoNPs, rather than the particles themselves, that led to cytotoxicity.

Furthermore, in order to evaluate the protective mechanism of bafilomycin A1 against CoNP-induced adverse biological reactions in RAW264.7 cells, we analyzed the ultrastructure of RAW264.7 cells by TEM and SEM. The SEM investigation indicated that RAW264.7 cells formed pseudopods when cultured in DMEM medium, but became rounded and did not spread when co-cultured with CoNPs. These observations

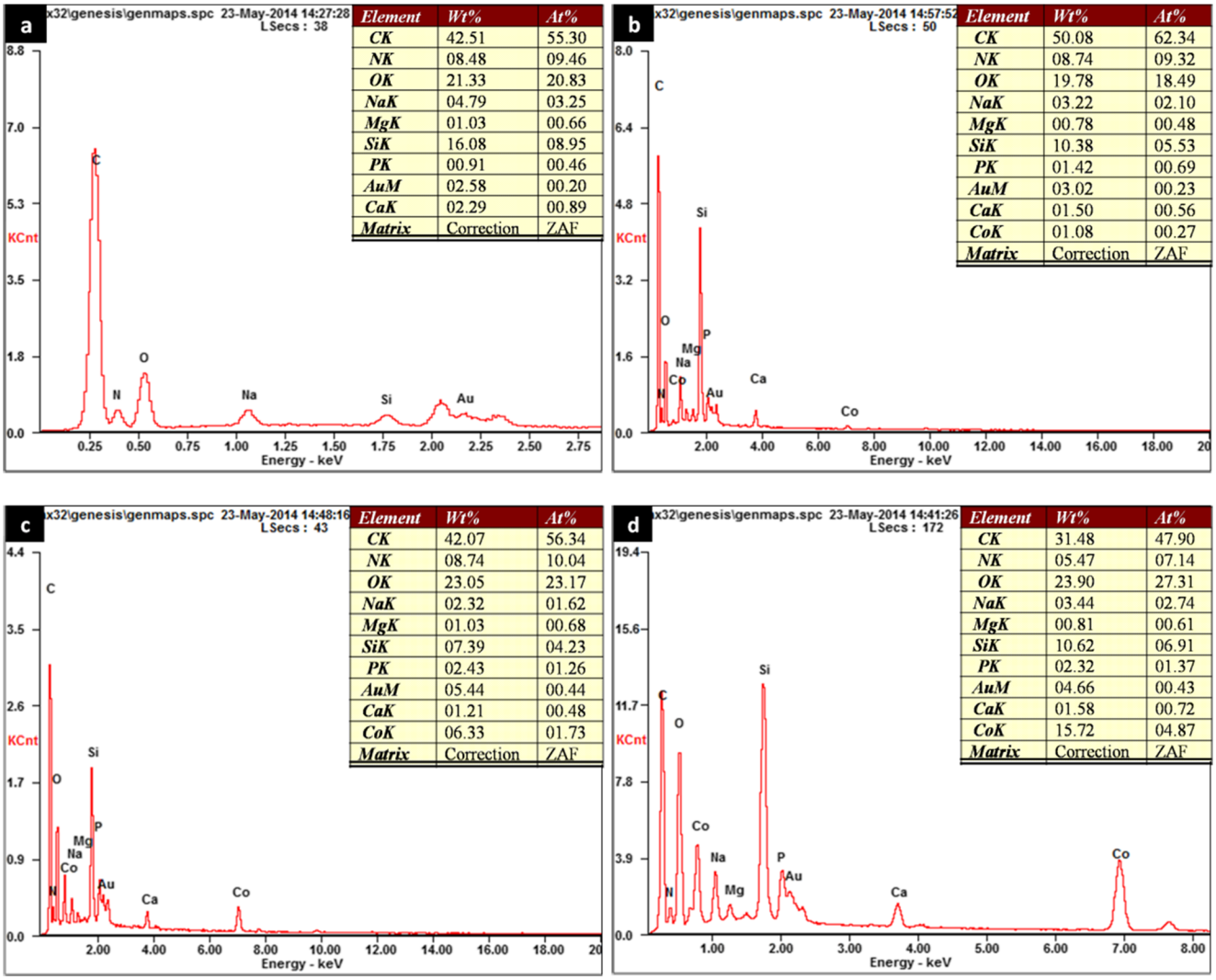

Fig. 6. Effects of bafilomycin A1 on the inhibition of intracellular solubilization of cobalt nanoparticles (CoNPs) analyzed by EDX. CoNPs (50 μM) were phagocytized by RAW264.7 cells. After 24 h of incubation in serum-free DMEM medium and isolation of cell extracts, the obtained pellets were analyzed by an energy dispersive spectrometer (EDX) assay. **a** Normal control group; **b** CoNPs-treated group; **c** CoNPs + 8 nM bafilomycin A1 group; **d** CoNPs + 16 nM bafilomycin A1 group

were in line with those of Jin et al. [28], who reported that L929 cells became round and shrank when co-cultured with TiO_2 nanoparticles. When pre-incubated with different concentrations of bafilomycin A1, the RAW264.7 cells dose dependently redeveloped pseudopods, their morphology recovered, and they again became able to spread. Taken together, these results indicated that CoNPs prevented cell proliferation and adhesion.

A recent study showed a 50- to 100-fold increased uptake of CoNPs compared with Co^{2+} [29]. CoNPs enter several types of cells quickly and easily via the clathrin-dependent pathway [13, 30]. Nanoparticles could easily be phagocytized and accumulate in the lysosomes and undergo intracellular dissolution by the "Trojan-horse"-type of mechanism, thereby inducing higher toxicity [31–33]. Su et al. [34] reported that ions released from intracellular nanoparticles created a "concentration effect," while Xia et al. [12] proposed that they created an "ion-wave" and exhibited much higher cytotoxicity. Our TEM images showed that, upon internalization, CoNPs were enclosed in lysosomes and vacuoles in RAW264.7 cells and that the number of lysosomes and vacuoles markedly increased, while some cytoplasmic organelles disappeared, upon exposure of the cells to the nanoparticles. Bafilomycin A1 can prevent a drop in pH within lysosomes, which significantly reduced the cobalt intracellular corrosion of CoNPs [13, 18], and reduce the "Trojan-horse"-type of release of large amounts of ions from CoNPs. TEM images showed that, when pre-incubated with bafilomycin A1, the TEM images showed the number of lysosomes and vacuoles decreased in a dose-dependent effect of bafilomycin A1, and cytoplasmic organelles reappeared.

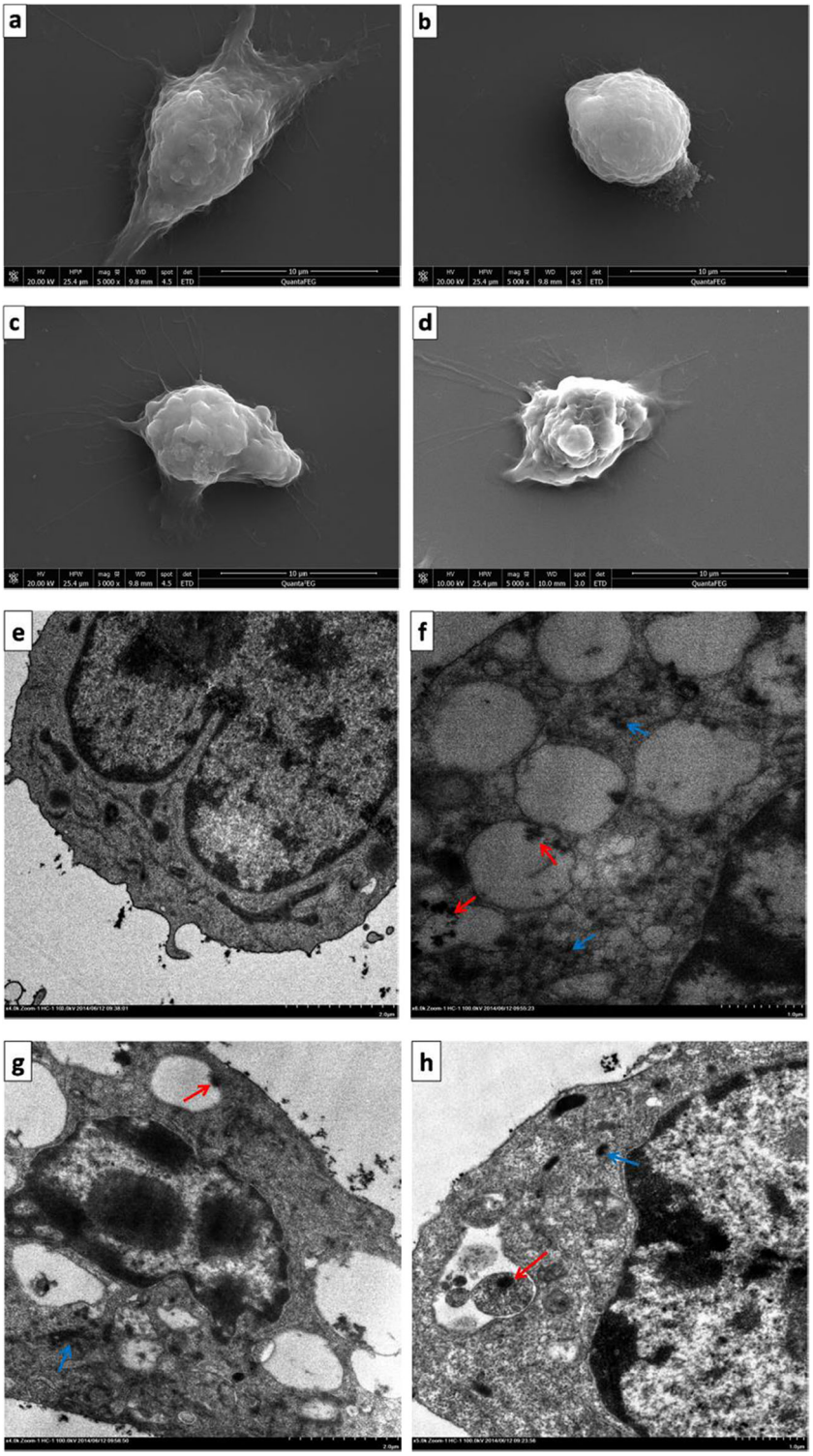

Fig. 7 Effects of bafilomycin A1 on the cell morphology of RAW264.7 cells. Cells were treated with cobalt nanoparticles (CoNPs; 50 μM). **a**–**d** scanning electron microscopy (SEM) micrograph; e–h transmission electron microscopy (TEM) micrograph; **a**, **e** Normal control group; b, f CoNPs-treated group; **c**, **g** CoNPs + 8 nM bafilomycin A1 group; **d**, **h** CoNPs + 16 nM bafilomycin A1 group; **f**, **g**, **h** the *blue arrows* indicate the CoNPs inside lysosomes and *red arrows* indicate the CoNPs inside vacuoles

Recent studies suggested that periprosthetic Co–Cr wear particles stimulated macrophage infiltration and phagocytosis, and the release of pro-inflammatory cytokines (TNF-α, IL-1β, IL-6, etc.) [35–40]. TNF-α, IL-1β, and IL-6 are known to promote the differentiation of precursor cells into mature osteoclasts, and are related to osteolysis [15, 41–45]. Considering that inhibition of intracellular corrosion of CoNPs by bafilomycin A1 could decrease the CoNP-induced cytotoxicity in RAW264.7 cells, we propose that bafilomycin A1 may have had protective effects against CoNP-induced aseptic

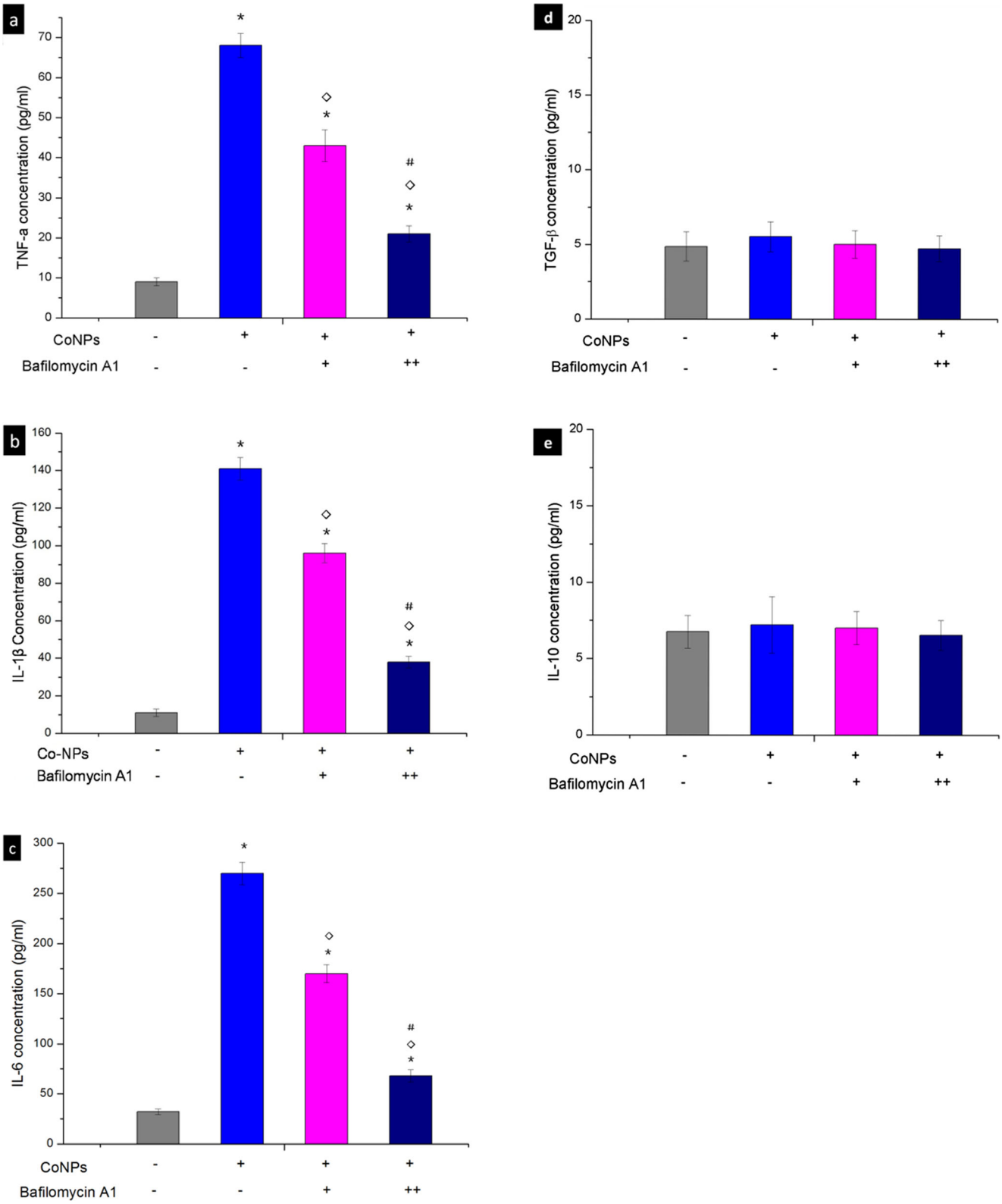

Fig. 8 Effects of bafilomycin A1 on pro-inflammatory cytokines and anti-inflammatory cytokines expression in cells in response to exposure to cobalt nanoparticles (CoNPs). TNF-α (**a**), IL-1β (**b**), IL-6 (**c**), TGF-β (**d**), and IL-10 (**e**) levels in the supernatants of tissue cultured cells after 24 h of incubation, as evaluated by ELISA. The results are shown as the mean ± SD of three independent experiments performed in triplicate. *$p < 0.05$ compared to control group; ◊$p < 0.05$ compared to CoNPs (20 μM)-treated group; #$p < 0.05$ compared to 8 nM bafilomycin A1 group

Table 1 Effects of bafilomycin A1 on the intracellular concentration of T-GSH/GSSG levels and antioxidant enzyme activities in RAW264.7 cells treated with cobalt nanoparticles (CoNPs; 20 μM)

	T-GSH (μM/mg protein)	GSSG	GSH/GSSG	T-SOD (U/mg protein)	GPx	CAT
Control	20.16 ± 2.02	6.56 ± 0.98	3.27 ± 1.01	113.46 ± 11.02	79.56 ± 3.98	96.57 ± 10.01
CoNPs	9.42 ± 1.27*	14.27 ± 1.51*	0.66 ± 0.52*	45.42 ± 5.17*	37.27 ± 6.21*	27.98 ± 4.52*
Plus 8 nM bafilomycin	13.18 ± 1.4$^{\diamond}$	13.29 ± 1.21$^{\diamond}$	0.99 ± 0.07$^{\diamond}$	78.13 ± 9.45$^{\diamond}$	42.59 ± 3.20$^{\diamond}$	56.07 ± 5.39$^{\diamond}$
Plus 16 nM bafilomycin	18.83 ± 2.14$^{\#}$	8.02 ± 0.89$^{\#}$	2.35 ± 0.86$^{\#}$	109.03 ± 10.25$^{\#}$	76.12 ± 4.76$^{\#}$	89.73 ± 9.82$^{\#}$

All data were expressed as mean ± SD of three independent experiments performed in triplicate

*GSH*glutathione, *GSSG* oxidized glutathione, *SOD* superoxide dismutase, *CAT* catalase, *GPx* glutathione peroxidase

$^{*}p < 0.05$ compared to control group; $^{\diamond}p < 0.05$ compared to CoNPs (20 μM)-treated group; $^{\#}p < 0.05$ compared to 8 nM bafilomycin A1 group

inflammation in RAW264.7 cells and could inhibit osteolysis. Up to 10 % of people with metal prostheses were found to have bone loss and implant loosening before 10 years of use [17, 46–49]; an innate macrophage inflammatory response to implant wear and corrosion products may be the primary cause of this phenomenon [17]. Given the toxicity of 50 μM CoNPs (IC50) and the reduced numbers of RAW264.7 cells available to secrete these cytokines[10], we chose to use a subtoxic concentration of CoNPs (20 μM) when we measured the release of pro-inflammatory cytokines in these cells. To our knowledge, this is the first report verifying that bafilomycin A1 could markedly inhibit the CoNP-induced inflammatory response and reduce the levels of the pro-inflammatory cytokines TNF-α, IL-1β, and IL-6 in a dose-dependent manner. Just as Shin [50] reported that wild panax ginseng and red-mold rice extracts induced IL-1α, IL-1β, IL-6, and TNF-α mRNA expression, but had no effect on IL-10 and TGF-β; in our study, the levels of TGF-β and IL-10 showed no obvious changes either co-cultured with subtoxic concentration of CoNPs or treated with bafilomycin A1; and further research work should be done in the future.

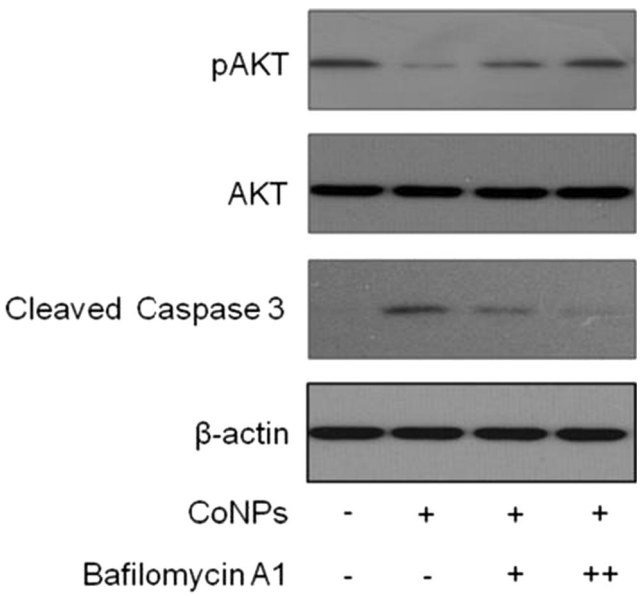

Fig. 9 Effects of bafilomycin A1 on pAKT, and cleaved caspase-3 expression in cells in response to cobalt nanoparticle (CoNP) exposure. Cells were pre-incubated for 4 h in the presence of different concentrations of bafilomycin A1 (0, 8, and 16 nM), and subsequently, the cells were exposed to 50 μM CoNPs or vehicle for 24 h. The treated cells were subjected to Western blot analysis with anti-pAKT, anti-AKT, and anti-caspase-3 antibody. β-actin levels demonstrate similar loading

The exact mechanisms by which cytotoxicity and aseptic inflammation are induced by CoNPs in vitro and in vivo remain unclear. Recent studies have found that nanoparticles induced toxicity through oxidative stress and inflammation by generating ROS in cells [3, 31]. Nanoparticles could induce intracellular oxidative stress by disturbing the balance between the oxidant and antioxidant processes [51, 52], but Liu et al. [53] proved that different nanoscale particles of similar sizes showed differences in toxicity, which could be attributed to their chemical compositions and shape. Further recent studies [54–56] proved that nanoscale ceramic materials were bioactive in cells and were less toxic than alloy nanoparticles. Park et al. [31] confirmed that adverse reactions were related to the physicochemical properties of nanoparticles. The characteristic of CoNPs that they could be easily dissolved in the low pH inside the lysosome most likely played a key role in inducing oxidative stress and inflammation. To verify that it was the Co^{2+} released from CoNPs during intracellular corrosion that induced oxidative stress, the effects on non-enzymatic and enzymatic antioxidant defense systems were monitored. In our study, T-GSH, T-SOD, CAT, and GPx levels of RAW264.7 cells were found to be significantly decreased after 24 h incubation with 20 μM CoNPs. These results were in line with those of Niska et al. [57], who reported that CuO nanoparticles can impair the antioxidant defense and decreased the levels of GSH, SOD, GST, or GPx in the mouse hippocampal HT22 cell line. When pre-incubated with different concentrations of bafilomycin A1, the activities of T-GSH, T-SOD, CAT, and GPx were restored in a dose-dependent manner. The inhibition of intracellular solubilization of CoNPs and the consequent reduction in Co^{2+} released inside cells by bafilomycin A1 may play an

important role in downregulating oxidative stress in RAW264.7 cells. Hence, it is likely that the Co^{2+} released from the intracellular corrosion of CoNPs, rather than the particles themselves, that lead to intracellular oxidative stress. Previous studies [58] showed that Co may downregulate Akt phosphorylation, and we hypothesized that the PI3K/Akt pathway may play a crucial role in the anti-apoptotic effect of bafilomycin A1 on CoNP-induced apoptosis. The levels of phosphorylated AKT and cleaved caspase-3 were examined by Western blot and showed that bafilomycin A1 triggered a rapid activation of Akt, which then initiated downstream signaling events including inhibiting apoptosis induced by CoNP.

There are several limitations of this study and several areas of further research could be identified. Although we minimized air contact time of cobalt nanoparticles to prevent oxidation reaction, but the formation of cobalt oxide nanoparticles may be inevitable [59]. Further research to evaluate if the heat-treatment would affect the outcome of such studies will be required in the future.

In conclusion, this study indicated that bafilomycin A1 could attenuate CoNP-induced toxicity and inflammation in RAW264.7 cells. The mechanisms are likely attributable to the inhibition of intracellular solubilization of CoNPs by bafilomycin A1, and the decreased Co^{2+} released inside cells plays a critical role in downregulation of oxidative stress inRAW264.7 cells.

Acknowledgments This study was funded by the National Natural Science Foundation of China (no. 81171743).

References

1. Smith J, Lee D, Bali K, Railton P, Kinniburgh D, Faris P, Marshall D, Burkart B, Powell J (2014) Does bearing size influence metal ion levels in large-head metal-on-metal total hip arthroplasty? A comparison of three total hip systems. J Orthop Surg Res 9:3
2. Jiang H, Liu F, Yang H, Li Y (2012) Effects of cobalt nanoparticles on human T cells in vitro. Biol Trace Elem Res 146:23–29
3. Avalos A, Haza AI, Mateo D, Morales P (2014) Cytotoxicity and ROS production of manufactured silver nanoparticles of different sizes in hepatoma and leukemia cells. J Appl Toxicol 34:413–423
4. Doorn PF, Campbell PA, Worrall J, Benya PD, McKellop HA, Amstutz HC (1988) Metal wear particle characterization from metal on metal total hip replacements: transmission electron microscopy study of periprosthetic tissues and isolated particles. J Biomed Mater Res 42:103–111
5. Queally JM, Devitt BM, Butler JS, Malizia AP, Murray D, Doran PP, O'Byrne JM (2009) Cobalt ions induce chemokine secretion in primary human osteoblasts. J Orthop Res 27:855–864
6. Stryker LS, Odum SM, Fehring TK, Springer BD (2015) Revisions of monoblock metal-on-metal THAs have high early complication rates. Clin Orthop Relat Res 473:469–474
7. Hwang KT, Kim YH, Kim YS, Choi IY (2013) Is second generation metal-on-metal primary total hip arthroplasty with a 28 mm head a worthy option?: a 12- to 18-year follow-up study. J Arthroplast 28:1828–1833
8. Kwon YM, Xia Z, Glyn-Jones S, Beard D, Gill HS, Murray DW (2009) Dose-dependent cytotoxicity of clinically relevant cobalt nanoparticles and ions on macrophages in vitro. Biomed Mater 4: 025018
9. Hart AJ, Quinn PD, Lali F, Sampson B, Skinner JA, Powell JJ, Nolan J, Tucker K, Donell S, Flanagan A, Mosselmans JF (2012) Cobalt from metal-on-metal hip replacements may be the clinically relevant active agent responsible for periprosthetic tissue reactions. Acta Biomater 8:3865–3873
10. Dalal A, Pawar V, McAllister K, Weaver C, Hallab NJ (2012) Orthopedic implant cobalt-alloy particles produce greater toxicity and inflammatory cytokines than titanium alloy and zirconium alloy-based particles in vitro, in human osteoblasts, fibroblasts, and macrophages. J Biomed Mater Res A 100:2147–2158
11. Xia Z, Triffitt JT (2006) A review on macrophage responses to biomaterials. Biomed Mater 1:R1–R9
12. Xia Z, Kwon YM, Mehmood S, Downing C, Jurkschat K, Murray DW (2011) Characterization of metal-wear nanoparticles in pseudotumor following metal-on-metal hip resurfacing. Nanomedicine 7:674–681
13. Ortega R, Bresson C, Darolles C, Gautier C, Roudeau S, Perrin L, Janin M, Floriani M, Aloin V, Carmona A, Malard V (2014) Low-solubility particles and a Trojan-horse type mechanism of toxicity: the case of cobalt oxide on human lung cells. Part Fibre Toxicol 11: 14
14. Raghunathan VK, Devey M, Hawkins S, Hails L, Davis SA, Mann S, Chang IT, Ingham E, Malhas A, Vaux DJ, Lane JD, Case CP (2013) Influence of particle size and reactive oxygen species on cobalt chrome nanoparticle-mediated genotoxicity. Biomaterials 34:3559–3570
15. Masui T, Sakano S, Hasegawa Y, Warashina H, Ishiguro N (2005) Expression of inflammatory cytokines, RANKL and OPG induced by titanium, cobalt-chromium and polyethylene particles. Biomaterials 26:1695–1702
16. Goodman SB, Huie P, Song Y, Schurman D, Maloney W, Woolson S, Sibley R (1998) Cellular profile and cytokine production at prosthetic interfaces. Study of tissues retrieved from revised hip and knee replacements. J Bone Joint Surg Br 80:531–539
17. Caicedo MS, Pennekamp PH, McAllister K, Jacobs JJ, Hallab NJ (2010) Soluble ions more than particulate cobalt-alloy implant debris induce monocyte costimulatory molecule expression and release of proinflammatory cytokines critical to metal-induced lymphocyte reactivity. J Biomed Mater Res A 93:1312–1321
18. Haynes DR, Rogers SD, Howie DW, Pearcy MJ, Vernon-Roberts B (1996) Drug inhibition of the macrophage response to metal wear particles in vitro. Clin Orthop Relat Res 323:316–326
19. Williams S, Tipper JL, Ingham E, Stone MH, Fisher J (2003) In vitro analysis of the wear, wear debris and biological activity of surface-engineered coatings for use in metal-on-metal total hip replacements. Proc Inst Mech Eng H J Eng Med 217:155–163
20. Wan R, Mo Y, Zhang X, Chien S, Tollerud DJ, Zhang Q (2008) Matrix metalloproteinase-2 and -9 are induced differently by metal nanoparticles in human monocytes: the role of oxidative stress and protein tyrosine kinase activation. Toxicol Appl Pharmacol 233: 276–285
21. Mak IT, Chmielinska JJ, Kramer JH, Weglicki WB (2009) AZT-induced oxidative cardiovascular toxicity: attenuation by Mg-supplementation. Cardiovasc Toxicol 9:78–85
22. Mak IT, Landgraf KM, Chmielinska JJ, Weglicki WB (2012) Angiotensin II promotes iron accumulation and depresses PGI_2 and NO synthesis in endothelial cells: effects of losartan and propranolol analogs. Can J Physiol Pharmacol 90:1413–1418

23. Zhang JQ, Shen M, Zhu CC, Yu FX, Liu ZQ, Ally N, Sun SC, Li K, Liu HL (2014) 3-Nitropropionic acid induces ovarian oxidative stress and impairs follicle in mouse. PLoS ONE 9: e86589.
24. Li HX, Xiao Y, Cao LL, Yan X, Li C, Shi HY, Wang JW, Ye YH (2013) Cerebroside C increases tolerance to chilling injury and alters lipid composition in wheat roots. PLoS ONE 8:e73380.
25. Rotruck JT, Pope AL, Ganther HE, Swanson AB, Hafeman DG, Hoekstra WG (1973) Selenium: biochemical role as a component of glutathione peroxidase. Science 179:588–590
26. Liao Y, Hoffman E, Wimmer M, Fischer A, Jacobs J, Marks L (2013) CoCrMo metal-on-metal hip replacements. Phys Chem Chem Phys 15:746–756
27. Darolles C, Sage N, Armengaud J, Malard V (2013) In vitro assessment of cobalt oxide particle toxicity: identifying and circumventing interference. Toxicol In Vitro 27:1699–1710
28. Jin CY, Zhu BS, Wang XF, Lu QH (2008) Cytotoxicity of titanium dioxide nanoparticles in mouse fibroblast cells. Chem Res Toxicol 21:1871–1877
29. Ponti J, Sabbioni E, Munaro B, Broggi F, Marmorato P, Franchini F, Colognato R, Rossi F (2009) Genotoxicity and morphological transformation induced by cobalt nanoparticles and cobalt chloride: an in vitro study in Balb/3T3 mouse fibroblasts. Mutagenesis 24: 439–445
30. Limbach LK, Wick P, Manser P, Grass RN, Bruinink A, Stark WJ (2007) Exposure of engineered nanoparticles to human lung epithelial cells: influence of chemical composition and catalytic activity on oxidative stress. Environ Sci Technol 41:4158–4163
31. Park EJ, Yi J, Kim Y, Choi K, Park K (2010) Silver nanoparticles induce cytotoxicity by a Trojan-horse type mechanism. Toxicol in Vitro 24:872–878
32. Cronholm P, Karlsson HL, Hedberg J, Lowe TA, Winnberg L, Elihn K, Wallinder IO, Möller L (2013) Intracellular uptake and toxicity of Ag and CuO nanoparticles: a comparison between nanoparticles and their corresponding metal ions. Small 9:970–982
33. Xia T, Kovochich M, Liong M, Mädler L, Gilbert B, Shi H, Yeh JI, Zink JI, Nel AE (2008) Comparison of the mechanism of toxicity of zinc oxide and cerium oxide nanoparticles based on dissolution and oxidative stress properties. ACS Nano 2:2121–2134
34. Su Y, Hu M, Fan C, He Y, Li Q, Li W, Wang LH, Shen P, Huang Q (2010) The cytotoxicity of CdTe quantum dots and the relative contributions from released cadmium ions and nanoparticle properties. Biomaterials 31:4829–4834
35. Hallab NJ, Jacobs JJ (2009) Biologic effects of implant debris. Bull NYU Hosp Jt Dis 67:182–188
36. Lewis JB, Randol TM, Lockwood PE, Wataha JC (2003) Effect of subtoxic concentrations of metal ions on NFkappaB activation in THP-1 human monocytes. J Biomed Mater Res A 64:217–224
37. Kaufman AM, Alabre CI, Rubash HE, Shanbhag AS (2008) Human macrophage response to UHMWPE, TiAlV, CoCr, and alumina particles: analysis of multiple cytokines using protein arrays. J Biomed Mater Res A 84:464–474
38. Campbell PA, Wang M, Amstutz HC, Goodman SB (2002) Positive cytokine production in failed metal-on-metal total hip replacements. Acta Orthop Scand 73:506–512
39. Catelas I, Petit A, Zukor DJ, Antoniou J, Huk OL (2003) TNF-alpha secretion and macrophage mortality induced by cobalt and chromium ions in vitro-qualitative analysis of apoptosis. Biomaterials 24:383–391
40. Thomas V, Halloran BA, Ambalavanan N, Catledge SA, Vohra YK (2012) In vitro studies on the effect of particle size on macrophage responses to nanodiamond wear debris. Acta Biomater 8:1939–1947
41. Ingham E, Fisher J (2005) The role of macrophages in osteolysis of total joint replacement. Biomaterials 26:1271–1286
42. Schwarz EM, Lu AP, Goater JJ, Benz EB, Kollias G, Rosier RN, Puzas JE, O'Keefe RJ (2000) Tumor necrosis factor-alpha/nuclear transcription factor-kappaB signaling in periprosthetic osteolysis. J Orthop Res 18:472–480
43. Algan SM, Purdon M, Horowitz SM (1996) Role of tumor necrosis factor alpha in particulate-induced bone resorption. J Orthop Res 14:30–35
44. Goodman SB, Ma T (2010) Cellular chemotaxis induced by wear particles from joint replacements. Biomaterials 31:5045–5050
45. Epstein NJ, Bragg WE, Ma T, Spanogle J, Smith RL, Goodman SB (2005) UHMWPE wear debris upregulates mononuclear cell pro-inflammatory gene expression in a novel murine model of intramedullary particle disease. Acta Orthop 76:412–420
46. Looney RJ, Schwarz EM, Boyd A, O'Keefe RJ (2006) Periprosthetic osteolysis: an immunologist's update. Curr Opin Rheumatol 18:80–87
47. Hallab NJ, Caicedo M, Finnegan A, Jacobs JJ (2008) Th1 type lymphocyte reactivity to metals in patients with total hip arthroplasty. J Orthop Surg Res 3:–6
48. Goodman SB (2007) Wear particles, periprosthetic osteolysis and the immune system. Biomaterials 28:5044–5048
49. Jacobs JJ, Hallab NJ (2006) Loosening and osteolysis associated with metal-on-metal bearings: a local effect of metal hypersensitivity? J Bone Joint Surg Am 88:1171–1172
50. Shin HM (2009) Mixture of wild panax ginseng and red-mold rice extracts activates macrophages through protection of cell regression and cytokine expression in methotrexate-treated RAW264.7 cells. J Korean Orient Med 30:69–79
51. Gurr JR, Wang AS, Chen CH, Jan KY (2005) Ultrafine titanium dioxide particles in the absence of photoactivation can induce oxidative damage to human bronchial epithelial cells. Toxicology 213: 66–73
52. Nel A, Xia T, Mädler L, Li N (2006) Toxic potential of materials at the nanolevel. Science 311:622–627
53. Liu H, Yang D, Yang H, Zhang H, Zhang W, Fang Y, Lin Z, Tian L, Lin B, Yan J, Xi Z (2013) Comparative study of respiratory tract immune toxicity induced by three sterilisation nanoparticles: silver, zinc oxide and titanium dioxide. J Hazard Mater 248-249:478–486
54. Zhang YF, Zheng YF, Qin L (2011) A comprehensive biological evaluation of ceramic nanoparticles as wear debris. Nanomedicine 7:975–982
55. Roualdes O, Duclos ME, Gutknecht D, Frappart L, Chevalier J, Hartmann DJ (2010) In vitro and in vivo evaluation of an alumina-zirconia composite for arthroplasty applications. Biomaterials 31:2043–2054
56. Tsaousi A, Jones E, Case CP (2010) The in vitro genotoxicity of orthopaedic ceramic (Al2O3) and metal (CoCr alloy) particles. Mutat Res 697:1–9
57. Niska K, Santos-Martinez MJ, Radomski MW, Inkielewicz-Stepniak I (2015) CuO nanoparticles induce apoptosis by impairing the antioxidant defense and detoxification systems in the mouse hippocampal HT22 cell line: protective effect of crocetin. Toxicol in Vitro 29:663–671
58. Catelas I, Petit A, Zukor DJ, Huk OL (2001) Cytotoxic and apoptotic effects of cobalt and chromium ions on J774 macrophages-implication of caspase-3 in the apoptotic pathway. J Mater Sci Mater Med 12:949–953
59. Rose SF, Weaver CL, Fenwick SA, Horner A, Pawar VD (2012) The effect of diffusion hardened oxidized zirconium wear debris on cell viability and inflammation—an in vitro study. J Biomed Mater Res B Appl Biomater 100:1359–1368